Denervation protects limbs from inflammatory arthritis via an impact on the microvasculature

Lars Stangenberg[a,1], Dalia Burzyn[b], Bryce A. Binstadt[b,2], Ralph Weissleder[a], Umar Mahmood[a,3], Christophe Benoist[b], and Diane Mathis[b,4]

[a]Center for Systems Biology, Massachusetts General Hospital, Harvard Medical School, Boston, MA 02114; and [b]Division of Immunology, Department of Microbiology and Immunobiology, Harvard Medical School, Boston, MA 02115

Contributed by Diane Mathis, June 10, 2014 (sent for review May 22, 2014)

Two-way communication between the mammalian nervous and immune systems is increasingly recognized and appreciated. An intriguing example of such crosstalk comes from clinical observations dating from the 1930s: Patients who suffer a stroke and then develop rheumatoid arthritis atypically present with arthritis on only one side, the one not afflicted with paralysis. Here we successfully modeled hemiplegia-induced protection from arthritis using the K/BxN serum-transfer system, focused on the effector phase of inflammatory arthritis. Experiments entailing pharmacological inhibitors, genetically deficient mouse strains, and global transcriptome analyses failed to associate the protective effect with a single nerve quality (i.e., with the sympathetic, parasympathetic, or sensory nerves). Instead, there was clear evidence that denervation had a long-term effect on the limb microvasculature: The rapid and joint-localized vascular leak that typically accompanies and promotes serum-transferred arthritis was compromised in denervated limbs. This defect was reflected in the transcriptome of endothelial cells, the expression of several genes impacting vascular leakage or transendothelial cell transmigration being altered in denervated limbs. These findings highlight a previously unappreciated pathway to dissect and eventually target in inflammatory arthritis.

inflammation | nervous system | vascular system | autoantibody

It has long been recognized that immune and inflammatory processes can be influenced by signals from the nervous system (1). For example, neuroendocrine hormones have well-known anti-inflammatory activities, first documented for corticosteroids in the arthritis context (2). Subsequently, motor neurons, the sympathetic nervous system (SNS), the parasympathetic nervous system (PNS), and sensory fibers have all been documented to modulate inflammation (3–5).

A striking example of nervous–immune system interaction comes from clinical observations made decades ago. As early as 1935, it was reported that patients who suffered a stroke and then developed rheumatoid arthritis (RA), often years after the neurologic insult, had an atypical disease presentation: Instead of the inflammatory symmetry typical of RA, only neurologically intact limbs developed joint inflammation (6). Later, this effect of central denervation was extended to peripheral denervation: Patients who were hemiplegic subsequent to polio or syphilis developed an analogous asymmetric arthritis (7, 8).

We set out to dissect this clinical phenomenon mechanistically by exploiting the power of the K/BxN T-cell receptor transgenic mouse model of inflammatory arthritis (9, 10). This model is particularly useful because of its easily distinguishable initiation and effector stages. The initiation phase relies primarily on the adaptive immune system. T lymphocytes displaying the transgene-encoded T-cell receptor recognize a self-peptide derived from GPI presented by the major MHC class II molecule, Ag7; these autoreactive T cells provide exceptionally effective help to GPI-specific B cells, resulting in massive, IL-17–dependent production of anti-GPI autoantibodies (autoAbs), primarily of the IgG1 isotype. The effector phase, which can be mimicked conveniently by transfer of serum from K/BxN into standard mice, is executed primarily by innate immune system players. GPI:anti-GPI immune complexes initiate a self-sustaining inflammatory response that mobilizes mast cells, neutrophils, perhaps macrophages, the alternative pathway of complement, Fc gamma receptors (FcγRs), TNF-α, IL-1, and others.

It proved possible to model hemiplegia-induced protection from arthritis in the K/BxN serum-transfer system: Serum recipients that had undergone unilateral transection of the sciatic and femoral nerves developed arthritis only in the paw on the innervated side. This finding prompted us to assess the roles of diverse elements of the nervous and allied systems in arthritis progression subsequent to serum transfer. Results from experiments using genetically deficient mouse strains and pharmacological inhibitors were unable to implicate a particular nerve quality but did point to a role for endothelial cells of the microvasculature. In accord, the endothelial cell transcriptomes of denervated and innervated ankles from K/BxN serum-transferred mice differed substantially and suggestively.

Results

Establishment of a Mouse Model of Asymmetric Arthritis Subsequent to Unilateral Paralysis. To enable mechanistic dissection of the arthritis-protective effect of hemiplegia, we adapted the K/BxN serum-transfer system. The hindpaw on one side of 6- to 8-wk-old C57BL/6 (B6) mice was denervated by transection of both the sciatic and femoral nerves, and the contralateral limb underwent a sham operation. Typically 10 d later, K/BxN serum was injected

Significance

Individuals who suffer paralysis on one side of the body and then develop rheumatoid arthritis show joint inflammation only on the neurologically intact side. We successfully modeled hemiplegia-induced protection from arthritis by transferring arthritogenic serum from K/BxN mice into recipients that had undergone unilateral sciatic and femoral nerve transection. Protection from serum-transferred arthritis could not be achieved by inhibiting the sympathetic, parasympathetic, or sensory arms of the nervous system. However, nerve transection did inhibit the joint-localized, inflammation-enhancing vascular leak rapidly induced by arthritogenic immune complexes and suggestively altered the transcriptome of the ankle microvasculature.

Author contributions: L.S., D.B., B.A.B., R.W., U.M., C.B., and D.M. designed research; L.S., D.B., and B.A.B. performed research; D.B., B.A.B., R.W., U.M., C.B., and D.M. analyzed data; and D.B. and D.M. wrote the paper.

The authors declare no conflict of interest.

[1]Present address: Beth Israel Deaconess Medical Center, Harvard Medical School, Boston, MA 02215.

[2]Present address: Center for Immunology, University of Minnesota, Minneapolis, MN 55414.

[3]Present address: Department of Radiology, Massachusetts General Hospital, Harvard Medical School, Boston, MA 02114.

[4]To whom correspondence should be addressed. Email: dm@hms.harvard.edu.

This article contains supporting information online at www.pnas.org/lookup/suppl/doi:10.1073/pnas.1410854111/-/DCSupplemental.

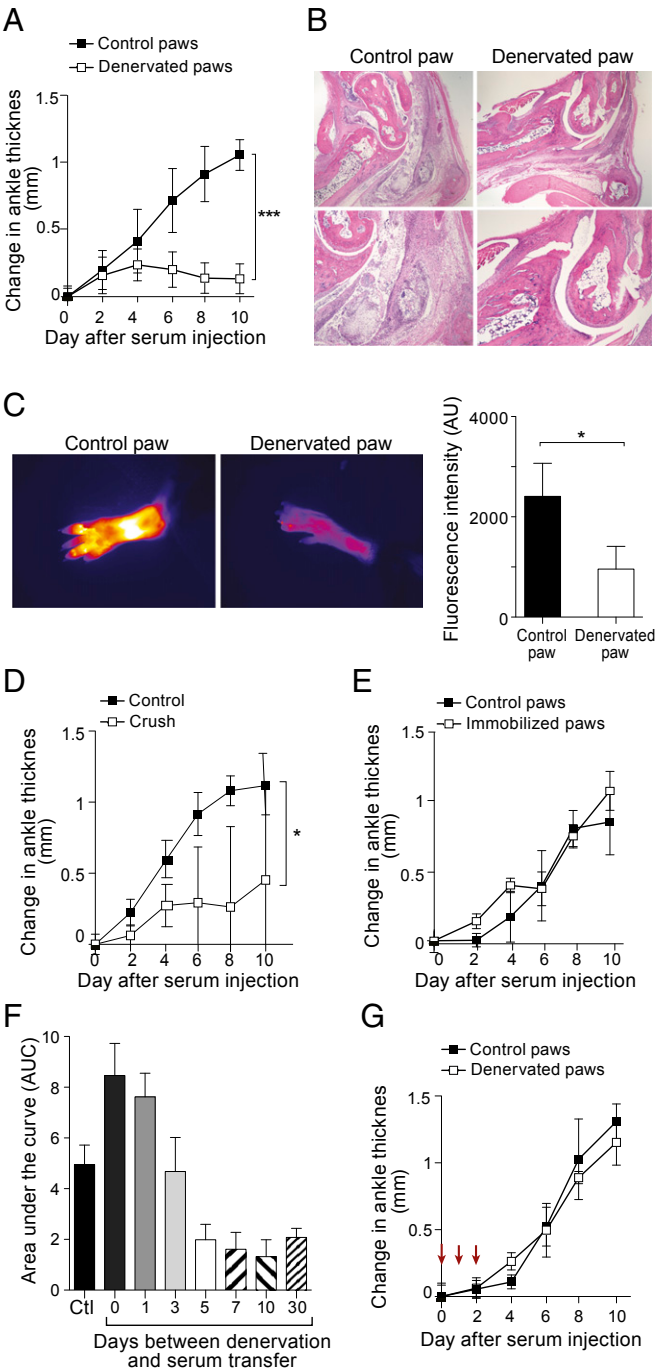

Fig. 1. Asymmetric arthritis after unilateral denervation. (*A*–*C*) B6 mice were subject to hindlimb denervation on one side and a sham operation on the other. Ten days later, they were injected with K/BxN serum (day 0), and arthritis was monitored over time by diverse assays. (*A*) Ankle swelling. Data shown are mean ± SD; ***$P < 0.001$ determined by Student *t* test; $n = 4$. (*B*) Histology. Analyzed by H&E staining 10 d after serum injection. (Magnification: *Upper*, 2×; *Lower*, 10×.) (*C*) Real-time protease imaging. A fluorescent cathepsin-B–activatable probe (ProSense) was injected on day 9 and imaged on day 10 after serum injection. (*Left*) Examples of images obtained with 2.7× magnification and color-coded in ImageJ with Fire. (*Right*) Summary quantification. Data shown are mean ± SD; *$P < 0.05$, determined by Student *t* test; $n = 4$. (*D*) Crush injury. Rather than surgical denervation, hindlimbs were subject to a milder crush, injury. Arthritis was induced and assayed as in *A*. *$P < 0.05$; $n = 3$. (*E*) Joint immobilization. Rather than surgical denervation, hindlimb joints were splint-immobilized. Arthritis was induced as in *A*. $n = 3$. (*F*) Impact of time since denervation. As in *A*, except varying intervals between surgery and serum transfer were tested. Area under the curve values are plotted; full curves can be found in Fig. S1. Ctl, sham-operated control. Data are shown as mean ± SD; $n = 4$. (*G*) Reversal of arthritis protection. As in *A*, except that IL-1β was i.p. injected on days 0, 1, and 2 (arrows) vis-à-vis serum transfer. $n = 4$.

i.p., usually twice, 2 d apart, and inflammatory arthritis was assessed over time.

As anticipated, control paws showed a steady augmentation of ankle thickness over the 10-d observation period; in contrast, denervated paws exhibited the usual increase only until day 2, after which there was little additional ankle thickening (Fig. 1*A*). Histologic examination at day 10 revealed the expected severe inflammation of control paws: a massive influx of neutrophils in periarticular tissues and within the synovial space and synovial hypertrophy (Fig. 1*B*, *Left*). These abnormalities were almost completely absent in the denervated paws (Fig. 1*B*, *Right*). Cathepsin B activity, another marker of inflammatory arthritis (11), also was greatly reduced in denervated paws, as indicated by minimal cleavage of a cathepsin-sensitive fluorescent nanoparticle injected on day 10 and monitored by noninvasive imaging (Fig. 1*C*). Nerve-crush injury, more mild than nerve transection, afforded protection as well, although such protection appeared to be less robust than that resulting from severance of the nerves (Fig. 1*D*).

To assess the importance of motor function in the serum-transfer system, we evaluated the effect of immobilizing hindpaws by application of a splint. This procedure did not confer protection from arthritis (Fig. 1*E*), although it is difficult to ensure absolute immobilization using such a strategy.

There was an intriguing time-dependence to the effect of denervation on the development of arthritis in the serum-transfer model. Concurrent nerve transection and serum injection paradoxically resulted in increased ankle swelling on the denervated compared with the innervated side (Fig. 1*F* and Fig. S1). With increasingly longer intervals between surgery and arthritis induction, this proinflammatory response converted to an anti-inflammatory, arthritis-protective mode, which was maintained for more than 1 mo after denervation (Fig. 1*F* and Fig. S1).

Last, we wondered whether the denervation-induced block to arthritis progression is reversible. Injection of a bolus of IL-1β can bypass genetic resistance to the arthritogenic power of K/BxN serum (12). IL-1β, administered on three consecutive days at the time of serum injection, completely reversed the arthritis block in denervated limbs, driving disease to the same level as in the innervated counterparts (Fig. 1*G*).

Comparison of the Transcriptomes of Control and Denervated Ankles. For additional insight into the aborted arthritis induced in the denervated limbs, we turned to genome-wide transcriptome analysis. We began by identifying gene-expression differences in whole-ankle tissue dissected from denervated and sham-operated limbs, independent of the response to K/BxN serum. Even 10 d post-surgery, the ankle-tissue transcriptomes diverged extensively: 238 genes were up-regulated, and 364 genes were down-regulated by at least twofold in the denervated samples ($P < 10^{-4}$, by permutation analysis) (Fig. 2*A* and Tables S1 and S2). These changes reflected a number of pathways involved in tissue homeostasis and development (see Fig. 2*B* for top pathway "hits" from Ingenuity analysis and Tables S3 and S4 for the actual genes involved), but the identity of these pathways yielded no obvious explanations for the arthritis-protective effect. Not surprisingly, and reassuringly, the transcripts most underrepresented in the denervated tissue encoded many myelin- and muscle-associated proteins (Table S2).

Subsequently, we compared gene-expression profiles of ankle tissue from denervated and innervated limbs after the administration of K/BxN serum. The analysis was focused on day 4 after serum transfer because this time point was the first to show a difference in ankle thickness and therefore might provide clues

to early defective processes, before secondary effects set in. Again the transcriptomes of denervated vs. innervated ankle tissue diverged significantly: 136 were up-regulated, and 241 genes were down-regulated in the denervated samples ($P < 10^{-4}$, by permutation analysis) (Fig. 2*C*). Superimposing on this plot the sets of transcripts over- or underrepresented in the absence of serum challenge (red and blue in Fig. 2*A*) revealed that most of the differential expression on day 4 after serum administration carried over from the prechallenged state (day 0). Few immunity- or inflammation-related genes made the twofold cutoff, notably the gene encoding SAA-1 did, an acute-phase reactant whose levels mount in blood and synovial fluid of arthritic humans and rodents (13) (Tables S5 and S6).

Assessment of the Contribution of Diverse Nerve Types to K/BxN Serum-Transferred Arthritis. We then sought to identify the type (s) of nerve involved in this model of inflammatory arthritis. The arthritis-protective effect detailed above was conferred by transection of the femoral and sciatic nerves, severing a variety of nerve types: motor, sympathetic, possibly parasympathetic, and sensory. First, we examined the impact of the two components of the vegetative nervous system, the SNS and PNS. The SNS seems to exert pro- or anti-inflammatory activity depending on the context, typically promoting inflammation at the outset of an immune response and reining it in at later stages (14). For example, blockade of β2 sympathetic signaling delayed the onset of antigen-induced arthritis and reduced its severity (3), whereas sympathectomy performed late in the course of collagen-induced arthritis worsened disease manifestations (15). To test the influence of the SNS in the K/BxN serum-transfer system, we administered, along with the serum, a set of pharmacologic agents that operate by a diversity of mechanisms. Guanethidine, a nonactive competitive inhibitor of norepinephrine at the presynaptic terminal, did not impact joint swelling; 6-hydroxydopamine, a potent neurotoxin, similarly failed to have an effect, as did reserpine, an irreversible norepinephrine reuptake inhibitor (Fig. 3*A*).

The PNS and its main anatomic correlate, the vagus nerve, have been linked to several inflammatory processes, usually exerting a dampening effect. For example, increased vagus nerve activity attenuated systemic sepsis, reducing levels of proinflammatory cytokines such as TNF-α, IL-1, and IL-6, whereas vagotomy exacerbated disease (5). The vagus nerve's anti-inflammatory function is mediated through acetylcholine (Ach) and a specific nicotinic Ach receptor, nAchRa7, which is present on macrophages and links the nervous and immune systems (16). The PNS was interrogated both via pharmacological inhibition and in KO mice. Coadministration of K/BxN serum and hexamethonium, a nondepolarizing ganglionic blocker, actually enhanced joint swelling (Fig. 3*B*, *Left*). On the other hand, mecamylamine, a nonselective and noncompetitive antagonist of nAchRs, did not change the course of disease (Fig. 3*B*, *Left*). Neither of these compounds is truly selective for the PNS, however; both inhibit SNS function as well. Therefore, as an independent test of the role of the PNS, we transferred serum into mice with a null mutation for *nAchRa7*. Arthritis developed as usual in these recipients (Fig. 3*B*, *Right*).

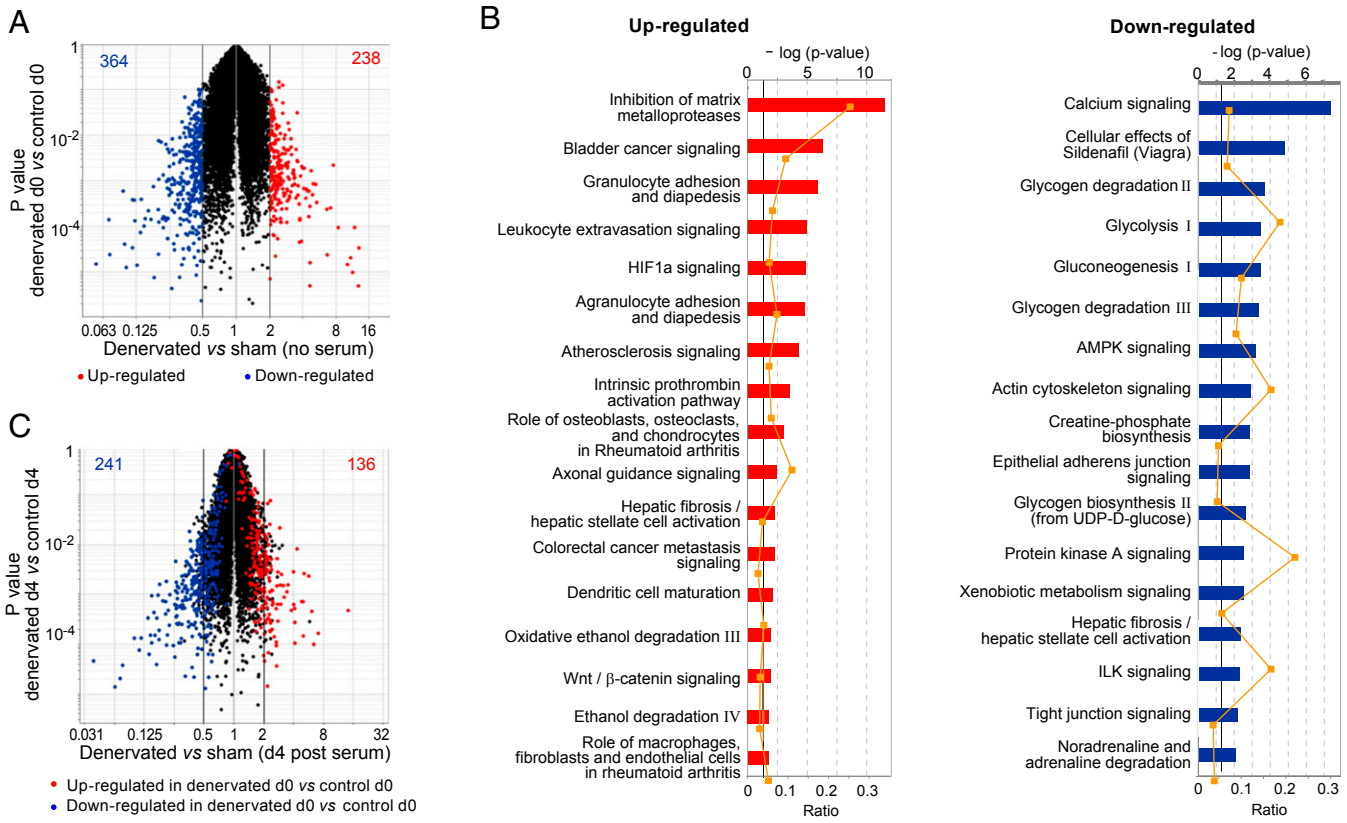

Fig. 2. Comparison of the transcriptomes of control and denervated ankles. Whole tissue from ankles of denervated or sham-operated limbs was dissected before or 4 d after induction of arthritis, and global gene expression was analyzed by microarray. (*A*) Volcano plot showing changes in gene expression induced by denervation in the absence of arthritis induction. (*B*) Canonical pathways (from Ingenuity) most enriched in sets of genes up- (*Left*) or down- (*Right*) regulated by denervation. The orange line indicates the ratio, calculated as the number of genes in a given pathway that meet cutoff criteria divided by total number of genes that make up that pathway. (*C*) Volcano plot comparing gene expression in denervated vs. control ankle tissue at day 4 after arthritis induction. Highlights represent genes up- (red) or down- (blue) regulated in denervated ankles in the absence of serum transfer (from *A*).

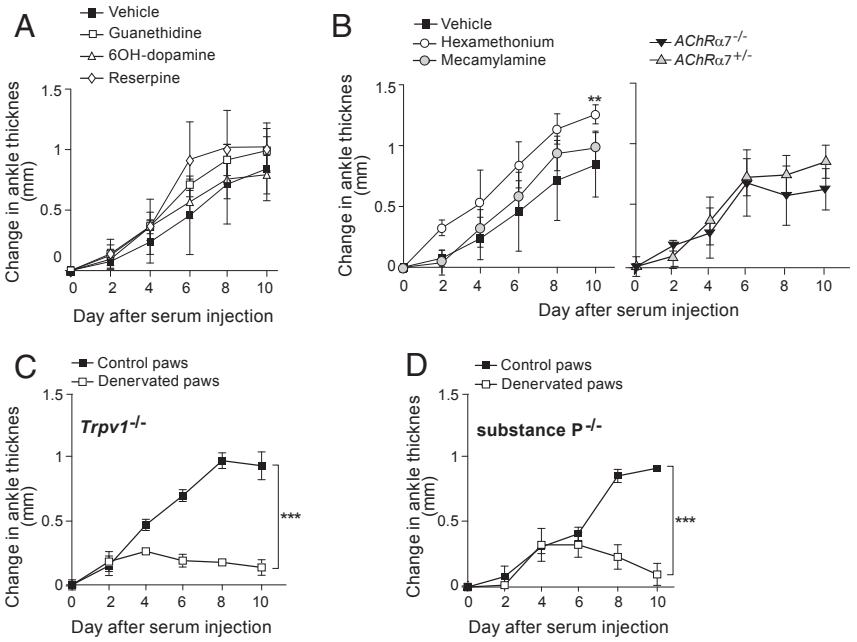

Fig. 3. Evaluation of the roles of various nerve types. (*A* and *B*) Role of the vegetative nervous system in K/BxN serum-transferred arthritis. Arthritis was induced and assayed in innervated limbs as in Fig. 1*A*. Pharmacological inhibitors of the SNS (*A*) or PNS (*B*, *Left*) were administered beginning on day 0, at the time of serum transfer. (*B*, *Right*) The response of *AchRα7*-KO mice and control littermates was tested. $^{**}P < 0.01$. (*C* and *D*) Role of sensory nerves in serum-transferred arthritis. Arthritis was induced and assayed in denervated or innervated hindlimbs as in Fig. 1*A*. The response of mice genetically deficient in Trpv-1 (*C*) or substance P (*D*) that had or had not been denervated was tested. $^{***}P < 0.001$; $n = 3$ for each condition.

Sensory fibers also can play an active role in inflammatory processes, expressing a variety of relevant receptors on their endings, including Toll-like, cytokine, prostaglandin, and catecholamine receptors (14). The transient receptor potential vanilloid cation channel 1 (TRPV1) is a proinflammatory nerve-fiber receptor that is activated by capsaicin (4). TPRV1 and like receptors are thought to sense activation of the immune system and to report the information to higher nerve centers in the spinal cord and brain. Subsequently, they release neuropeptides such as substance P and calcitonin gene-related peptide-1 (CGRP-1), which have powerful vasodilatory and chemotactic properties and thereby can prime the local environment for an inflammatory response (17, 18). To assess the influence of sensory nerves on K/BxN serum-transferred arthritis, we tested mice bearing a null mutation for TRPV1 or for substance P. Transfer of serum into each of these KO strains could provoke inflammatory arthritis with the usual course, and disease could be inhibited by denervation (Fig. 3 *C* and *D*).

Demonstration of Effects on the Microvasculature. We showed previously that K/BxN serum-transferred arthritis induces and depends on a rapid and joint-localized increase in microvascular permeability, a process that requires histamine and serotonin (19). There are manifold links between the nervous and vascular systems: For example, VEGF, a major stimulant of angiogenesis, also promotes axon growth (20); the SNS and PNS control cardiovascular parameters such as blood pressure and heart rate; and the neurovascular unit, a term encompassing endothelial cells, neurons, astrocytes, pericytes, and extracellular matrix, is increasingly recognized as central to neurodegenerative diseases (21). Hence, we quantified vascular leakage in denervated and sham-operated limbs of K/BxN-serum recipients. Using a noninvasive, real-time method for visualizing the vasculature of live mice via confocal microscopy of a long-circulating intravascular imaging probe (19), we found a clear reduction and delay in the vessel leakage that typically occurs minutes after serum injection (Fig. 4 *A* and *B*). Because systemic administration of histamine or serotonin had been shown previously to trigger analogous joint-localized vasopermeability in limbs of standard mice, i.e., to mimic the effect of GPI:anti-GPI immune complexes, we checked whether this triggering also occurred in denervated limbs. It did not, suggesting a defect in endothelial cell sensing (Fig. 4*C*).

Given the clear impact of denervation on the vasculature of serum-transferred mice and the lack of reversal by vasoactive amines, we looked for mechanistic clues in the transcriptomes of hindpaw endothelial cells. Tie2-GFP mice, in which endothelial cells are fluorescently tagged, were subjected to denervation or a sham operation. After 10 d, hindpaw endothelial cells were purified by flow cytometry, RNA was isolated, and gene expression was profiled using Affymetrix microarrays. To focus on genes relevant to vascular permeability, we generated a transendothelial migration signature using information from the Gene-Set Enrichment Analysis (GSEA) Molecular Signature Database (MSigDB) and the Ingenuity database (listed in Table S7). Superimposition of this signature onto a plot comparing the transcriptomes of denervated and innervated hindpaw endothelial cells revealed a significant underrepresentation of these transcripts in the denervated hindpaw (Fig. 4*D*). The genes most differentially expressed (Table S7) include representatives of several signaling pathways critical for regulating vascular permeability (Fig. S2).

Discussion

The major goals of this study were to establish a mouse model for hemiplegia-induced protection from RA and to exploit this model to elucidate the mechanistic underpinnings of this fascinating, but little explored, clinical phenomenon. We turned to the well-studied K/BxN serum-transfer system, which mimics many of the clinical and immunological features of human inflammatory arthritis (22). The impact of denervation on the response to arthritogenic serum by mice was astonishingly parallel to the effect of central or peripheral denervation on subsequent RA development by humans. For example, in both cases, denervation is initially proinflammatory, but a long-lasting anti-inflammatory state eventually sets in (Fig. 1*D* and ref. 23). Because of the simplicity of the serum-transfer system, focused on the arthritis effector phase, and because of its tractability to experimental manipulation, easily adapted for genetic or pharmacologic intervention, we could evaluate candidate systems, pathways, and molecules rapidly. Several of our observations merit further discussion.

First, the surgical procedure, which injures nerve fibers of the motor, SNS, PNS, and sensory systems, resulted in extensive,

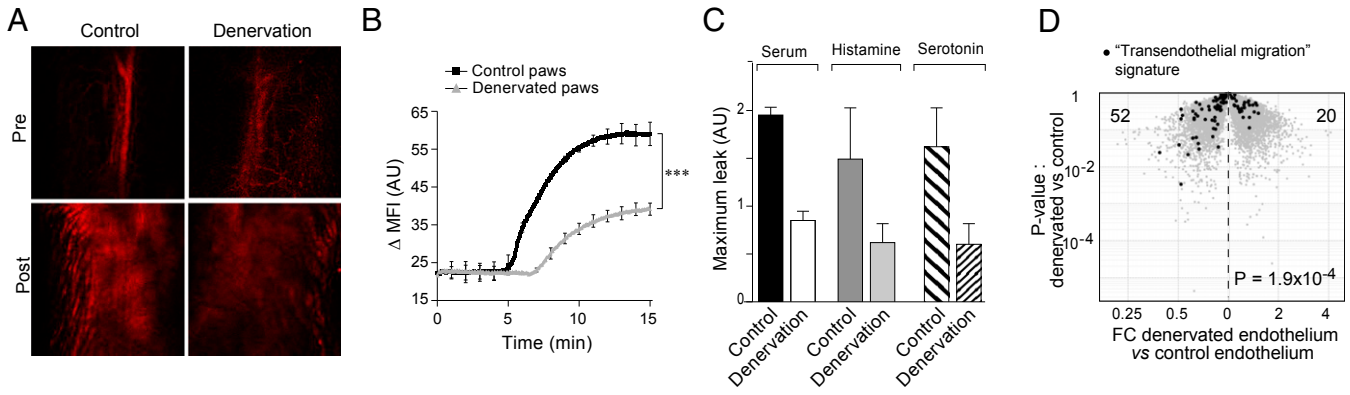

Fig. 4. Effects of hindlimb denervation on the ankle microvasculature. (*A–C*) Inhibition of K/BxN serum-induced vascular leak. The vascular probe AngioSense 680 was i.v. injected 5 min before serum transfer. (*A*) Single-plane confocal micrographs of control and denervated hindpaws just before and 10 min after serum injection. (Magnification: 10×.) (*B*) Quantification of the change in mean fluorescence intensity (ΔMFI) of confocal micrographs obtained every 5 s for 15 min after serum injection. ΔMFI was calculated vis-à-vis the preserum value. Data shown are representative of four mice. ***$P < 0.001$, calculated by the Student *t* test. (*C*) Effect of injecting vasoactive amines instead of serum on vascular leak in innervated vs. denervated hindpaws. $n = 3–4$. (*D*) Changes in endothelial cell transcriptome. Microarray analysis of gene expression by endothelial cells isolated from paws of denervated or sham-operated limbs. Genes from a transendothelial migration signature (Table S7) are highlighted on a volcano plot. *P* value was determined by a χ^2 test.

long-lasting transcriptome changes in the denervated limb, independent of serum transfer. The damage caused by transection of the sciatic and femoral nerves causes what is known as "Wallerian degeneration" (24). Nerve fibers distal to the injury undergo rapid degeneration, with only the sheath remaining to guide regenerative axon sprouting; some retraction of proximal fibers also occurs. At the cellular level, the distal degeneration is dominated by a massive accumulation of macrophages, peaking between days 7 and 14 and then gradually clearing (25). At the molecular level, there is an increase in perineural levels of proinflammatory mediators such as TNF-α, IL-1β, CCL2, and CCL3, even before the expansion of the macrophage population, i.e., at days 1–3 (26, 27). Thus, the denervation-induced transcriptome changes must reflect a complex mix of cellular and molecular responses, of both a degenerative and regenerative nature, as well as more distal effects. Most striking, although not unexpected, was the underrepresentation in the denervated limbs of a group of myelin-related and muscle-associated transcripts and the overrepresentation of transcripts related to tissue regeneration.

Second, we were unable to identify a particular nerve quality required for K/BxN serum-transferred arthritis. This finding contrasts with previous reports of an effect of manipulating the SNS in other mouse models of inflammatory arthritis (sometimes via the same inhibitors) (3, 15). A likely explanation for the divergent results is that the models previously interrogated are rather different: Unlike the K/BxN serum-transfer system, they encompass both the initiation and effector stages of arthritis and depend on the injection of an adjuvant to induce disease. We only can surmise that in the system we used the overall, integrated, quantity or quality of nerve signaling is the critical parameter or, alternatively, that the denervation procedure damaged auxiliary systems.

Third, hindpaw denervation did result in vascular changes known to be detrimental to the progression of arthritis. The K/BxN serum-transferred disease is preceded by and depends on a rapid increase in joint-localized macromolecular permeability of the microvasculature (19, 28). Anti-GPI autoAbs are recognized by FcγRIII, likely on mast cells, which in turn release histamine and serotonin, thereby provoking a transient increase in vascular permeability. Consequently, more anti-GPI autoAbs exit the circulation and deposit in the joints, and more innate immune cells gain access to the periarticular space. Anti-GPI–induced vascular leak was significantly delayed and reduced in denervated hindpaws. Interestingly, unlike the case for control paws, injection of histamine or serotonin into denervated paws did not elicit joint-localized vascular permeability. Because these vasoactive amines bypass the need for anti-GPI, neutrophils, mast cells, and FcγRIII, this result pointed to a possible defect in endothelial cells of the joint.

Indeed, expression of a number of genes implicated in controlling vascular permeability was altered, either negatively or positively, in the endothelium of denervated hindpaws. Among the down-regulated genes whose products promote vessel permeability and cell transmigration are *Axl* and *Jam2*. Axl is a tyrosine kinase crucial in the VEGF-A pathway, downstream of PI3K/AKT activation; *Axl*-null mice showed reduced permeability in several inflammatory contexts (29). Junctional adhesion molecule 2 (encoded by *Jam2*) is an endothelial cell-surface protein that promotes rolling and adhesion of immune cells, a prerequisite for transmigration (30); blockade of this protein abrogated transmigration of primary human peripheral blood leukocytes across umbilical vein endothelial cells (31).

Among the up-regulated genes encoding proteins known to dampen endothelial leak and cellular transmigration are *Argptl4* and *Cry61*. Angiopoietin-like 4, structurally similar to the angiopoietins, protects vascular integrity in contexts of myocardial infarction and tumor metastasis; *Angptl4*-KO mice showed altered VEGFR2/VE-cadherin complexes and disrupted endothelial cell adherens junctions (32, 33). Cysteine-rich angiogenic inducer 61 (encoding by *Cr61*), produced by fibroblasts and endothelial cells, is considered an important matrix protein promoting tissue repair and immune cell adhesion by binding various integrins; high expression of this molecule inhibits transmigration of innate and adaptive immune cells (34). Clearly, transcriptome changes in hindpaw endothelial cells support the notion that vascular alterations in the denervated limbs reduce access to arthritogenic cells and molecules.

Such a scenario makes evolutionary sense. Paralyzed limbs are prone to venous and lymphatic stasis, because of the lack of motor activity, which normally acts as a pump to return blood and lymph centrally to the heart and thoracic duct. Therefore the limb tends to become edematous, increasing the likelihood of microbial infections. Minimizing vascular leak would result in less edema and, thereby, fewer infections.

Materials and Methods

Mice. Male mice (6- to 8-wk-old) of the following strains were purchased from Jackson Laboratory: C57BL/6J, Tie2 reporter (Tg(TIE2GFP)287Sato/J), substance P-deficient (B6.Cg-Tac1tm1Bbm/J), TRPV-deficient (B6.129 × 1-Trpv1tm1Jul/J), and nAchRa7-deficient (B6.129S7-Chrna7tm1Bay/J) mice. All mouse procedures were approved by the institutional subcommittee on research animal care at Massachusetts General Hospital.

Denervation and Arthritis Induction. On the same leg, the sciatic nerve was isolated in the gluteal fossa posteriorly and the femoral nerve was isolated anteriorly distal to the inguinal ligament. Denervation was accomplished by transection and removal of at least 2 mm of nerve. Sham operations were performed on the contralateral leg.

K/BxN serum-transferred arthritis was induced by i.p. injection of 150 μL pooled serum from 8-wk-old K/BxN mice on days 0 and 2. For arthritis reversal, 100 μg of IL-1β was injected i.p. on days 0, 1, and 2. Clinical arthritis was assessed by measuring ankle thickness.

For histological analysis, animals were killed at the indicated time points, and paws were harvested. After decalcification with 9% (vol/vol) formic acid, specimens were processed using standard paraffin embedding and were stained with H&E.

Protease Imaging. Imaging of a fluorescent cathepsin-B–sensitive probe (Prosense; Perkin-Elmer) was performed as described (11). Mice were injected with the probe 9 d after serum treatment and were imaged 1 d later. Images were processed with ImageJ (National Institutes of Health) to define regions of interest and to color-code using Fire filter.

Microarray Analysis. For whole-ankle gene expression, hindpaws of B6 mice were harvested at various time points in the course of disease and prepared as previously described (35). For endothelial cell gene expression, hind paws of Tie2-GFP mice were harvested 10 d after denervation and prepared as above. Cells then were sorted on the GFP signal and directly collected in TRIzol (Life Technologies). All cell populations were generated in triplicate.

RNA was processed and analyzed using M430 2.0 chips (Affymetrix) as detailed previously (35) and updated (36). The analysis of canonical pathways used Ingenuity Pathway Analysis (IPA; Ingenuity Systems). The transendothelial migration signature was generated by extracting gene sets relevant to this function from IPA and MSigDB (www.broad.mit.edu/gsea).

Pharmacological Manipulation. Compounds were diluted in normal saline to the specified concentration and were administered as follows: guanethidine at 0.5 mg daily i.p., 6-OH-dopamine at 80 mg/kg every other day i.p., reserpine at 5 mg/kg every other day i.p., hexamethonium at 5 $mg \cdot kg^{-1} \cdot h^{-1}$ s.c., and mecamylamine at 1 mg/kg daily orally. Administration began on day 0, at the time of serum transfer.

Confocal Imaging of Vessel Permeability. Vascular imaging was performed as previously described (19) after injection of AngioSense 680 (Perkin-Elmer) into serum-transferred or histamine (200 mg/kg)- or serotonin (10 mg/kg)-injected mice. Microscopy was performed with a multichannel upright confocal microscope (Radiance 2100; Bio-Rad Laboratories).

Statistical Analysis. Statistical analysis was performed using the program Prism 5 (GraphPad Software). One-way ANOVA and the Student *t* test were performed as indicated in the figure legends.

ACKNOWLEDGMENTS. This work was funded by National Institutes of Health Grant AI054904 (to D.M., C.B., and R.W.). L.S. was supported by a fellowship from the Deutsche Forschungsgemeinschaft, STA 1025/1-1, and B.A.B. was supported by a Pfizer Postdoctoral Fellowship in Rheumatology/Immunology.

1. Eskandari F, Webster JI, Sternberg EM (2003) Neural immune pathways and their connection to inflammatory diseases. *Arthritis Res Ther* 5(6):251–265.
2. Kass EH, Finland M (1951) The role of adrenal steroids in infection and immunity. *N Engl J Med* 244(13):464–470.
3. Levine JD, Coderre TJ, Helms C, Basbaum AI (1988) Beta 2-adrenergic mechanisms in experimental arthritis. *Proc Natl Acad Sci USA* 85(12):4553–4556.
4. Alawi K, Keeble J (2010) The paradoxical role of the transient receptor potential vanilloid 1 receptor in inflammation. *Pharmacol Ther* 125(2):181–195.
5. Borovikova LV, et al. (2000) Vagus nerve stimulation attenuates the systemic inflammatory response to endotoxin. *Nature* 405(6785):458–462.
6. Coste F, Forestier M (1935) Hemiplegie et nodosities d'Heberden contralaterales. *Bull Mem Soc Med Hop Paris* 51:772–776.
7. Jacqueline F (1953) [A case of evolutive polyarthritis with localisation controlateral to a hemiplegia]. *Rev Rhum Mal Osteoartic* 20(4):323–324.
8. Thompson M, Bywaters EG (1962) Unilateral rheumatoid arthritis following hemiplegia. *Ann Rheum Dis* 21:370–377.
9. Kouskoff V, et al. (1996) Organ-specific disease provoked by systemic autoimmunity. *Cell* 87(5):811–822.
10. Monach PA, Mathis D, Benoist C (2008) The K/BxN arthritis model. *Curr Protoc Immunol* Chapter 15 Unit 15.22.
11. Ji H, et al. (2002) Arthritis critically dependent on innate immune system players. *Immunity* 16(2):157–168.
12. Nigrovic PA, et al. (2007) Mast cells contribute to initiation of autoantibody-mediated arthritis via IL-1. *Proc Natl Acad Sci USA* 104(7):2325–2330.
13. Zhang N, Ahsan MH, Purchio AF, West DB (2005) Serum amyloid A-luciferase transgenic mice: Response to sepsis, acute arthritis, and contact hypersensitivity and the effects of proteasome inhibition. *J Immunol* 174(12):8125–8134.
14. Pongratz G, Straub RH (2013) Role of peripheral nerve fibres in acute and chronic inflammation in arthritis. *Nat Rev Rheumatol* 9(2):117–126.
15. Härle P, Möbius D, Carr DJ, Schölmerich J, Straub RH (2005) An opposing time-dependent immune-modulating effect of the sympathetic nervous system conferred by altering the cytokine profile in the local lymph nodes and spleen of mice with type II collagen-induced arthritis. *Arthritis Rheum* 52(4):1305–1313.
16. Wang H, et al. (2003) Nicotinic acetylcholine receptor alpha7 subunit is an essential regulator of inflammation. *Nature* 421(6921):384–388.
17. Carolan EJ, Casale TB (1993) Effects of neuropeptides on neutrophil migration through noncellular and endothelial barriers. *J Allergy Clin Immunol* 92(4):589–598.
18. Saban MR, Saban R, Bjorling D, Haak-Frendscho M (1997) Involvement of leukotrienes, TNF-alpha, and the LFA-1/ICAM-1 interaction in substance P-induced granulocyte infiltration. *J Leukoc Biol* 61(4):445–451.
19. Binstadt BA, et al. (2006) Particularities of the vasculature can promote the organ specificity of autoimmune attack. *Nat Immunol* 7(3):284–292.
20. Ruiz de Almodovar C, et al. (2011) VEGF mediates commissural axon chemoattraction through its receptor Flk1. *Neuron* 70(5):966–978.
21. Zlokovic BV (2011) Neurovascular pathways to neurodegeneration in Alzheimer's disease and other disorders. *Nat Rev Neurosci* 12(12):723–738.
22. Sachithanandan N, et al. (2011) Macrophage deletion of SOCS1 increases sensitivity to LPS and palmitic acid and results in systemic inflammation and hepatic insulin resistance. *Diabetes* 60(8):2023–2031.
23. Nava P (1953) [Old rheumatoid arthritis; cerebral ictus; acute evolutive outbreak of pain in joints of the hemiplegic side]. *Bras Med* 67(16-17):318–321.
24. Luo L, O'Leary DD (2005) Axon retraction and degeneration in development and disease. *Annu Rev Neurosci* 28:127–156.
25. Mueller M, et al. (2003) Macrophage response to peripheral nerve injury: The quantitative contribution of resident and hematogenous macrophages. *Lab Invest* 83(2):175–185.
26. Perrin FE, Lacroix S, Avilés-Trigueros M, David S (2005) Involvement of monocyte chemoattractant protein-1, macrophage inflammatory protein-1alpha and interleukin-1beta in Wallerian degeneration. *Brain* 128(Pt 4):854–866.
27. Shamash S, Reichert F, Rotshenker S (2002) The cytokine network of Wallerian degeneration: Tumor necrosis factor-alpha, interleukin-1alpha, and interleukin-1beta. *J Neurosci* 22(8):3052–3060.
28. Wipke BT, Wang Z, Kim J, McCarthy TJ, Allen PM (2002) Dynamic visualization of a joint-specific autoimmune response through positron emission tomography. *Nat Immunol* 3(4):366–372.
29. Ruan GX, Kazlauskas A (2012) Axl is essential for VEGF-A-dependent activation of PI3K/Akt. *EMBO J* 31(7):1692–1703.
30. Ludwig RJ, et al. (2005) Junctional adhesion molecules (JAM)-B and -C contribute to leukocyte extravasation to the skin and mediate cutaneous inflammation. *J Invest Dermatol* 125(5):969–976.
31. Johnson-Léger CA, Aurrand-Lions M, Beltraminelli N, Fasel N, Imhof BA (2002) Junctional adhesion molecule-2 (JAM-2) promotes lymphocyte transendothelial migration. *Blood* 100(7):2479–2486.
32. Galaup A, et al. (2006) Angiopoietin-like 4 prevents metastasis through inhibition of vascular permeability and tumor cell motility and invasiveness. *Proc Natl Acad Sci USA* 103(49):18721–18726.
33. Galaup A, et al. (2012) Protection against myocardial infarction and no-reflow through preservation of vascular integrity by angiopoietin-like 4. *Circulation* 125(1):140–149.
34. Löbel M, et al. (2012) CCN1: A novel inflammation-regulated biphasic immune cell migration modulator. *Cell Mol Life Sci* 69(18):3101–3113.
35. Jacobs JP, et al. (2010) Deficiency of CXCR2, but not other chemokine receptors, attenuates autoantibody-mediated arthritis in a murine model. *Arthritis Rheum* 62(7):1921–1932.
36. Burzyn D, et al. (2013) A special population of regulatory T cells potentiates muscle repair. *Cell* 155(6):1282–1295.